MODELLING OF NON-DRAG FORCES FOR BUBBLY FLOWS

Dirk Lucas, Jun-Mei Shi, and Eckhard Krepper

1. Introduction

Interfacial force closure is one of the central topics in Eulerian multiphase flow modelling. In vertical bubbly flow, the non-drag forces, namely the lift, wall, turbulent dispersion and added mass force, play the most important role in calculating the gas concentration distribution. These forces have a complex nature. Generally their magnitudes depend on the bubble size. Moreover, it is found that the lift force changes its sign with increasing bubble diameter [1,2]. For this reason, a wall gas peak is observed for small bubbles in comparison with a central peak for larger bubbles in vertical co-current upflows [3,4]. In an air-water system at ambient conditions, the change of the direction of the lift force in the shear field occurred at a bubble diameter of 5.8 mm. Therefore, one has to consider an inhomogeneous multi-size class model in order to correctly predict the gas distribution in a poly disperse flow [5,6].

Non-drag force models were implemented in CFX-5.6 and validated using the experimental database for air-water flow in a vertical pipe (inner diameter 51.2 mm), established at FZR using wire-mesh sensor technology. Bubble size distributions as well as radial profiles of the gas volume fraction, represented by bubbles of different size were measured. A simplified model [4] was also used to test a number of these models in an extended range of parameters.

2. Non-drag bubble forces

The non-drag forces discussed here are: lift force, wall force and turbulent dispersion force. The **lift force** considers the interaction of the bubble with the shear field of the liquid. Related on the unit volume it can be calculated as:

$$\vec{F}_L = -C_L \rho_l (\vec{w}_g - \vec{w}_l) \times rot(\vec{w}_l) \tag{1}$$

The classical lift force, which has a positive coefficient C_L , acts in the direction of decreasing liquid velocity, i.e. in case of co-current upwards pipe flow in the direction towards the pipe wall. Numerical [1] and experimental [2] investigations showed, that the direction of the lift force changes its sign, if a substantial deformation of the bubble occur. Tomiyama et al. [2] conducted investigations on single bubbles and derived a correlation for the coefficient of the lift force C_L from these experiments. This coefficient depends on the Eötvös number, which is proportional to the square of the bubble diameter. For the water-air system at normal conditions C_L changes its sign at an bubble diameter of d_b = 5.8 mm. Bubble diameter in this paper always means the equivalent bubble diameter regarding the volume of a sphere.

The **wall lubrication force**, which pushes the bubbles away from the wall, was first introduced by Antal [7]. A modified formulation was introduced by Tomiyama et al. [2]:

$$\vec{F}_W = -C_W \frac{d_{bubb}}{2} \left(\frac{1}{y^2} - \frac{1}{(D-y)^2} \right) \rho_l w_{rel}^2 \vec{n}_r \tag{2}$$

They also proposed a correlation for the coefficient, which again depends on the Eötvös number [2]. Later a modified correlation for this coefficient was published [8]. It was used in our investigations together with a bubble deformation force, introduced in [9].

The **turbulent dispersion force** is the result of the turbulent fluctuations of liquid velocity. Lahey et al. [10] derived an equation for the force per unit volume as

$$\vec{F}_{TD} = -C_{TD}\rho_l k_l \ \mathrm{grad}\,\alpha \text{, with } C_{TD} = 0.1. \quad (3)$$

Burns [11] derived an equation from the fluctuations of the drag force by Favre averaging procedure (FAD model):

$$\vec{F}_{TD} = -\frac{3C_D \nu_{t,l}}{4 d_b \,\mathrm{Pr}} \frac{\rho_l w_{rel}}{1-\alpha} \mathrm{grad}\,\alpha \qquad = -C_{TD}^{FAD} \rho_l k_l \ \mathrm{grad}\,\alpha, with \qquad C_{TD}^{FAD} = \frac{3C_D \nu_{t,l}}{4 d_b k_l \,\mathrm{Pr}} \frac{w_{rel}}{1-\alpha} \quad (4)$$

The turbulent Prandtl number (or Schmidt number) has an order of magnitude of 1. Similar expressions were derived earlier by a number of authors, e.g. by Gosman et al. [12].

3. Validation of non-drag force models using the simplified model

The simplified model for vertical pipe flow introduced in [4] was used to test and to validate the different models for the non-drag forces. It considers a large number of bubble classes. The model bases on the assumption of an equilibrium of the non-drag forces. This assumption is valid as good approximation at the upper end of the investigated pipe. The model solves the radial profiles of liquid and gas velocities, bubble-size class resolved gas fraction profiles as well as turbulence parameters on basis of a given bubble size distribution. The Sato model [13] is used to calculate the radial profile of the liquid velocity and the turbulent viscosity required as an input for the models for the forces (see eq. (1),(4)). Because of the strong interaction between the radial profiles of the liquid velocity and the gas volume fraction, an iteration procedure is used. The model was extended to consider the dimension of the bubbles [9]. The lateral extension of the bubble is especially important for large bubbles. All equations describing the forces acting on bubbles are derived for parameters present at the position of the centre of mass of the bubble. The bubble itself is an object with a considerable extension in space, i.e. the distributions found for an equilibrium of the forces have to be transformed into gas fraction distributions by convoluting them with a geometry function characteristic for the lateral gas fraction distribution of a bubble.

Fig. 1 compares measured and calculated radial gas volume fraction profiles for selected combinations of superficial velocities. The profiles were calculated using lift and wall forces according to eq. (1) and (2) with correlations for the coefficients from Tomiyama et al. and different dispersion forces. The red curves accord to the model introduced in [4]. Here for the turbulent dispersion force eq. (3) was used. In addition an Eötvös number dependend dispersion force was introduced. It increases with the Eötvös number without any limitation, what provokes the flat profiles for large bubbles and slugs, which occur in the case of low liquid and high gas superficial velocities. Using the dispersion FAD model, eq. (4) for these points radial gas fraction profiles with pronounced peaks in the pipe centre and at wall occur (green curves). This is due to the non-considered effect of the extension of the large bubbles and slugs. By consideration of the bubble dimensions, these deviations from the measured profiles vanish (blue curves). In general the agreement between calculated and measured profiles is satisfactory despite for liquid superficial velocity of 4 m/s. Because of the strong gradient of the liquid velocity the lift force causes a pronounced wall peak in the calculation, while the measurements show an intermediate peak of the radial gas volume fraction. Investigations on bubble forces were also done for other variations of the dispersion force as well as for different wall force models.

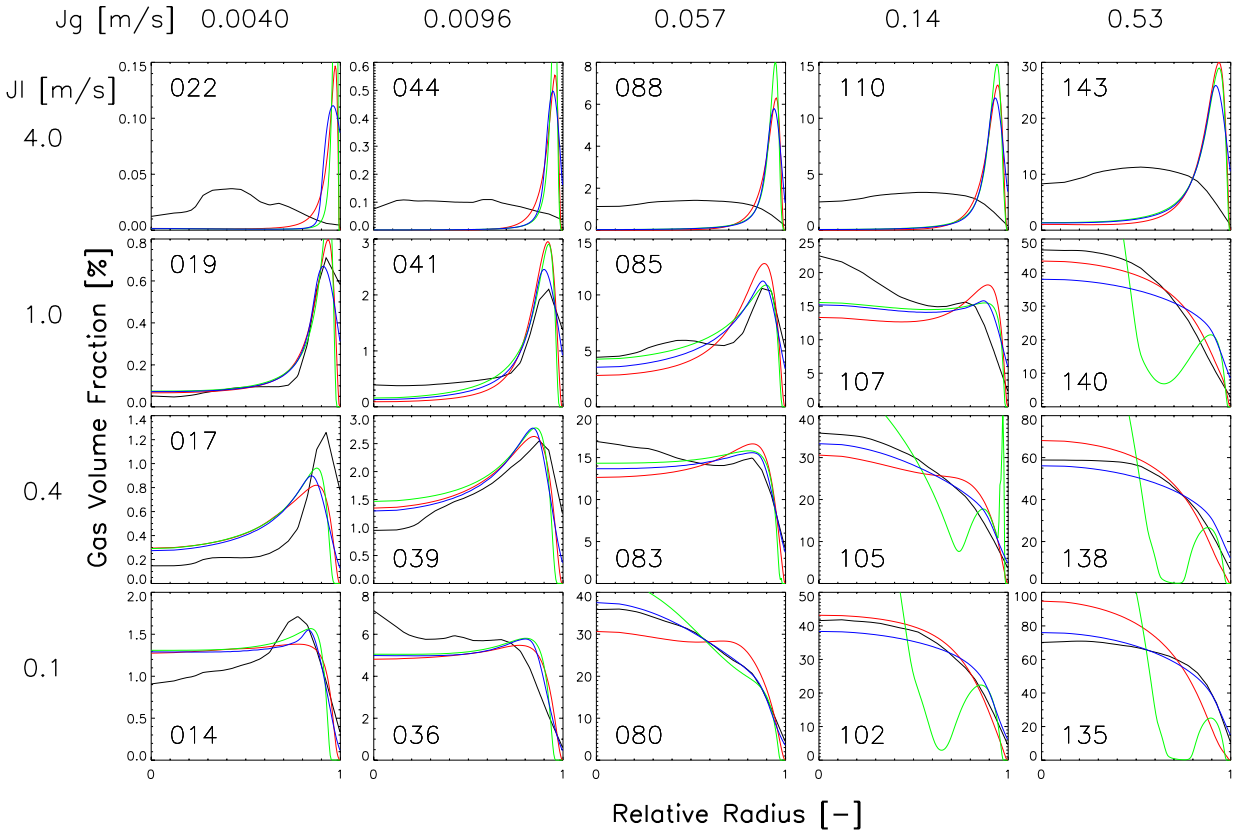

Fig. 1: Effect of different dispersion force models: ▬ *Experiment,* ▬ *model in [4],* ▬ *Eq. (4)* ▬ *Eq. (4) and consideration of bubble dimension.*

4. Implementation and validation of non-drag force models in CFX-5.6

A number of non-drag force models available in literature were implemented via CFX USER ROUTINE and CFX command language in collaboration with ANSYS CFX Germany. Moreover, detailed validations were carried out for these models using the experimental database. Based on the present work, several non-drag force models are now available in CFX-5.7. Especially, the FAD model, eq. (4) has been implemented as the default turbulent dispersion force model in CFX-5.7 Eulerian multiphase flow package [11]. Details of the work were reported in Shi et al. [14], Frank et al. [15] and Burns et al. [11]. In addition, inspired by the success of the FAD model, an alternative model derivation was provided, which bridges the Eulerian and Lagrangian approach. Concepts were also proposed to improve the turbulent dispersion force model, eq. (3) by taking into account the bubble induced turbulence.

For the validation, a number of test cases in the bubbly flow regime were defined. A computational domain consisting of a 3 degree sector of the pipe with the symmetry condition on both sector faces was applied in the simulation. The numerical simulation was based on the CFX-5.6 two-fluid model. Both fluids were assumed to be incompressible and one constant bubble diameter was assumed within the total computational domain. The Shear Stress Transport (SST) turbulence model [16] was applied to the continuous phase. Bubble induced turbulence was accounted for following the enhanced eddy viscosity model of Sato [13]. The dispersed phase turbulence was treated assuming a simple algebraic relationship between the dispersed phase and continuous phase kinematic eddy viscosities. The interfacial forces are

considered by the Grace model for the drag force, the Tomiyama correlations for the lift and wall lubrication force [2], and either the FAD model or eq. (3) with C_{TD} = 0.35 for the turbulence dispersion force. The added mass force was neglected for the stationary flow considered here. Details on the convergence error, grid dependence of the results and the inlet condition effect are reported in Shi et al. [14]. Numerical results for the normalized air volume fraction profiles, defined by

$$\alpha_g^* = \frac{\alpha_g}{\alpha_{g,0}}, \text{ with } \quad \alpha_{g,0} = 2\int_0^1 \alpha_g(r^*) r^* dr^* \tag{5}$$

were compared against the wire-mesh measurement data at L/D = 59.2 (Fig. 2). It can be observed that all numerical results based on the FAD model agree fairly well with the experimental data. It is observed from Fig. 2 that the gas volume fraction obtained using eq. 3 is consistently lower in the core region than those based on the FAD model (eq. 4). This indicates a stronger turbulence dispersion force given by the latter. The FAD model leads to much better agreements with the experimental data in certain cases, such as FZR-074, though the core gas concentration is still underpredicted. This deviation can be reduced by using two fluids for the gas phase, namely separating the larger bubbles (negative lift force) from the small ones. This will be the subject of future investigation.

Fig. 3 shows the the corresponding turbulence dispersion force coefficient of the FAD model C_{TD}^{FAD} (see eq. 4). The results clearly show that the turbulent dispersion force given by eq. 3 is much too weak, except in the near-wall region. Moreover, Fig. 3 also shows that a constant coefficient C_{TD} as assumed in eq. 3 is not realistic. In addition, it is interesting to note that C_{TD} decreases with increasing superficial velocity of the continuous phase. This is because the bubble response time τ_d is similar for all test cases due to their similar d_p, whereas the turbulence time scale τ_t decreases with increasing flow Reynolds numbers.

Table 1: Test cases used for the validation

No.	J_L [m/s]	J_G [m/s]	d_b [mm]	No.	J_L [m/s]	J_G [m/s]	d_b [mm]
017	0,405	0,0040	4,8	040	0,641	0,0096	4,6
019	1,017	0,0040	4,8	041	1,017	0,0096	4,5
038	0,255	0,0096	4,3	042	1,611	0,0096	3,6
039	0,405	0,0096	4,5	074	1.017	0,0368	4.5

5. Conclusions

A number of non-drag force models were implemented in CFX-5.6. Careful validations were carried out based on FZR MTLOOP experimental data base. The FAD Model has been shown to lead to better agreements with the measurement data for most of the test cases and to be numerically more robust than the model given by eq. (3). Consequently, it has been implemented as the default model of choice for turbulence dispersion in CFX-5.7.

Acknowledgements

This work is the result of a strong collaboration between Forschungszentrum Rossendorf and ANSYS-CFX Germany. Financial support is gratefully acknowledged from the Ministry of Economy and Labour (BMWA) of Germany in the project “TOPFLOW – Transient two phase flow test facility for generic investigation of two-phase flows and further development and validation of CFD codes”.

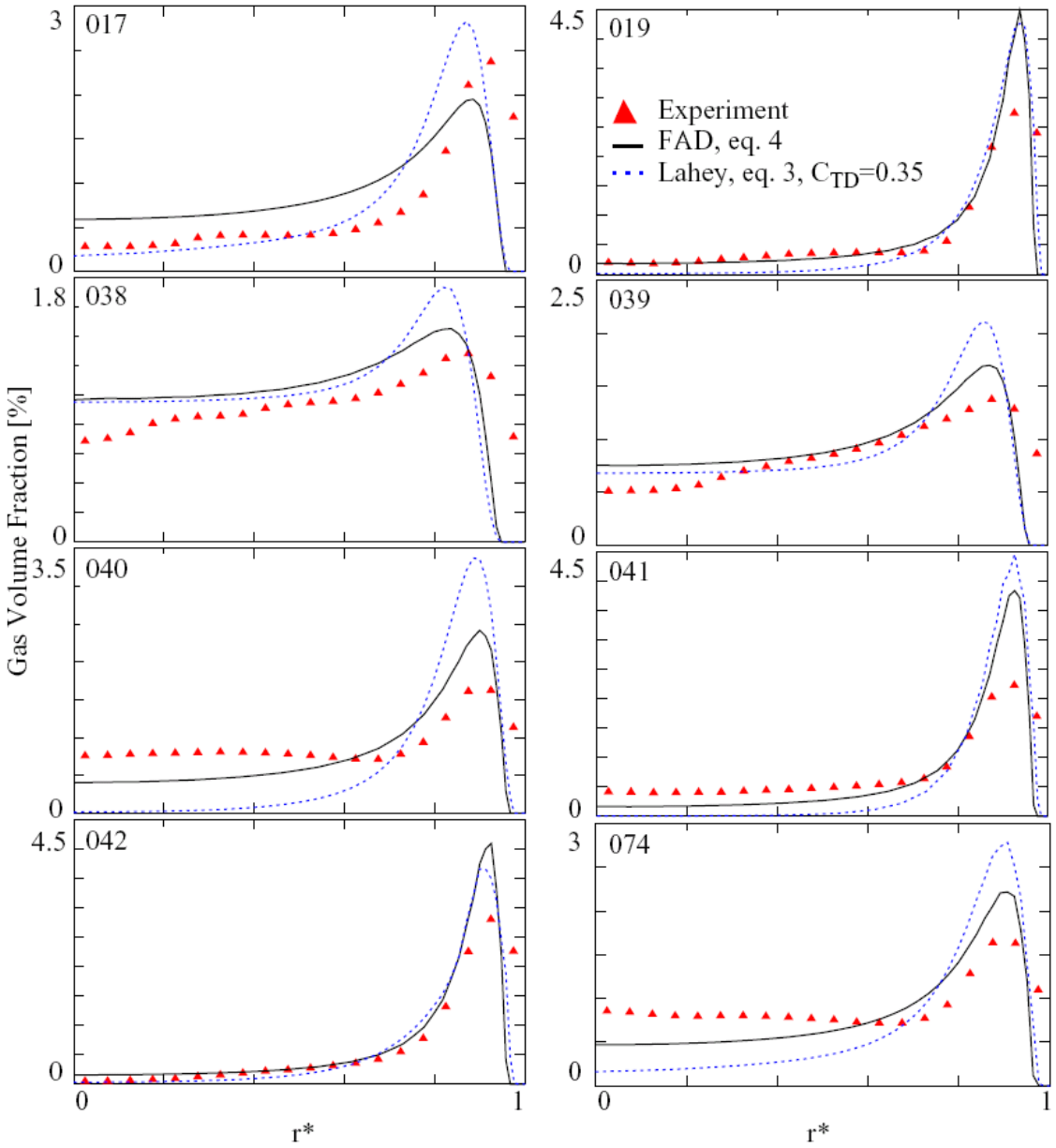

Fig. 2: Comparisons between FAD model (eq.4) and eq. 3 for the test cases defined in Tab. 1.

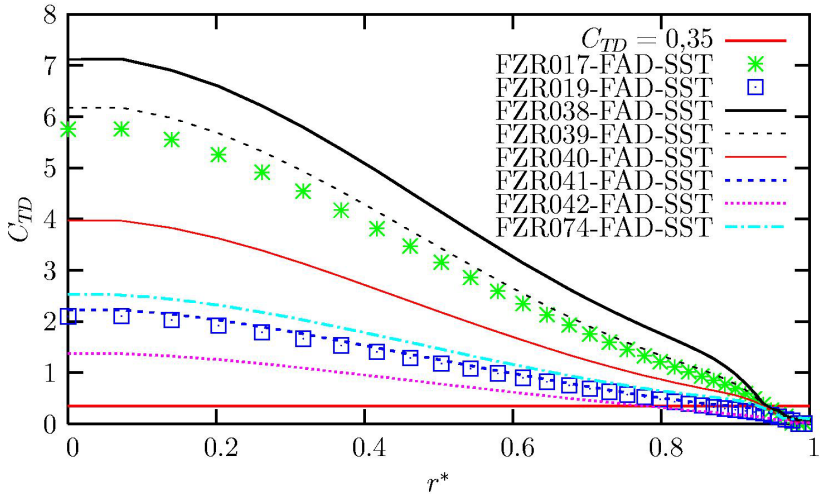

Fig. 3: Equivalent C_{TD} coefficient of FAD model in comparison with constant coefficient eq. 3.

References

[1] E.A. Ervin, G. Tryggvason, The rise of bubbles in a vertical shear flow, Journal of Fluids Engineering, vol. 119, pp. 443-449, 1997.

[2] A. Tomiyama, A. Sou, I. Zun, N. Kanami, T. Sakaguchi, Effects of Eötvös number and dimensionless liquid volumetric flux on lateral motion of a bubble in a laminar duct flow, Advances in Multiphase Flow, pp. 3-15, 1995.

[3] H.-M. Prasser, E. Krepper, D. Lucas, Evolution of the two-phase flow in a vertical tube - decomposition of gas fraction profiles according to bubble size classes using wire-mesh sensors, Int. J. of Thermal Sciences, vol. 41, pp. 17-28 (2002).

[4] D. Lucas, E. Krepper, H.-M. Prasser, Prediction of radial gas profiles in vertical pipe flow on basis of the bubble size distribution, International *J. of Thermal Sciences*, vol. 40, pp. 217-225, 2001.

[5] D. Lucas, E. Krepper, H.-M. Prasser, Modelling of bubble flow in vertical pipes, The 10th Int. Topical Meeting on Nuclear Reactor Thermal Hydraulics (NURETH-10), Seoul, Korea, paper A00301, 2003.

[6] J.-M. Shi, E. Krepper, D. Lucas, U. Rohde, Some concepts for improving the MUSIG model. Internal note Forschungszentrum Rossendorf, March 2003

[7] S.P. Antal, R.T. Lahey, J.E. Flaherty, Analysis of phase distribution in fully developed laminar bubbly two-phase flow, *Int. J.l of Multiphase Flow*, vol. 7, pp. 635-652, 1991.

[8] S. Hosokawa, A. Tomiyama, S. Misaki, T. Hamada, Lateral migration of single bubbles due to the presence of wall, *Proceedings of ASME Fluids Engineering Division Summer Meeting*, Montreal, Ouebec, Canada, 2002.

[9] D. Lucas, J.-M. Shi, E. Krepper, H.-M. Prasser, Models for the forces acting on bubbles in comparison with experimental data for vertical pipe flow, 3rd International Symposium on Two-Phase Flow Modelling and Experimentation, Pisa, Italy, September 22-24, 2004

[10] R.T. Lahey, M. Lopez de Bertodano, O.C. Jones, Phase distribution in complex geometry conduits, Nuclear Engineering and Design, vol. 141, pp. 177-201, 1993.

[11] A.D. Burns, T. Frank, I. Hamill, J.-M. Shi, The favre averaged drag model for turbulence dispersion in Eulerian multi-phase flows, *5th Int. Conf. on Multiphase Flow,* Paper No. 392, *ICMF'2004*, Yokohama, Japan, 2004.

[12] A.D. Gosman, C. Lekakou, S. Politis, R.I. Issa, M.K. Looney, Multidimensional modeling of turbulent two-phase flow in stirred vessels, AIChE Journal, vol. 38, pp. 1946-1956, 1992.

[13] Y. Sato, M. Sadatomi, K. Sekoguchi, Momentum and heat transfer in two-phase bubble flow-I, *Int. J. of Multiphase Flow*, vol. 7, pp. 167-177, 1981.

[14] J.-M. Shi, Th. Frank, E.Krepper, D. Lucas, U. Rohde, H.-M. Prasser, Implementation and validation of non-drag interfacial forces in CFX-5.6, *5th Int. Conf. on Multiphase Flow,* Paper No. 400, *ICMF'2004*, Yokohama, Japan, 2004.

[15] Th. Frank, J.-M. Shi, A. Burns, Validation of Eulerian multiphase flow models for nuclear safety applications, 3rd Int. Symposium on Two-Phase Flow Modeling and Experimentation, Pisa, Italy, September 22-24, 2004.

[16] F.R. Menter, Two-equation eddy-viscosity turbulence models for engineering applications, *AIAA-Journal*, Vol. 32, No. 8., 1994.